



Consistent long-term observations of surface phytoplankton functional types from space

Hongyan Xi^{1*}, Marine Bretagnon², Ehsan Mehdipour^{1,3}, Julien Demaria², Antoine Mangin², Astrid Bracher^{1,4}

5 ¹Alfred Wegener Institute, Helmholtz-Centre for Polar and Marine Research, Bremerhaven, 27570, Germany

²ACRI-ST, Sophia Antipolis Cedex, France

³School of Business, Social & Decision Sciences, Constructor University, Bremen, Germany

⁴Institute of Environmental Physics, University of Bremen, Bremen, 28359, Germany

Correspondence to: Hongyan Xi (hongyan.xi@awi.de)

10 **Abstract.** Global products of phytoplankton functional types (PFTs) derived from multi-sensor ocean color data provide important long-term biogeochemical quantifications indexed by chlorophyll *a* concentration (Chla) of PFTs including diatoms, haptophytes, prokaryotic phytoplankton, dinoflagellates, and green algae. Due to the distinctive lifespans and radiometric characteristics of ocean color sensors, the consistency of the PFT products derived from different sensors needs to be assured to establish a complete and systematic frame for long-term monitoring of multiple PFTs on a global scale. This study introduces

15 a machine learning (ML) based correction scheme to eliminate the discrepancies between different sensors' PFT products. The correction scheme is applied to the OLCI-derived PFT data, to match them with the merged sensor-derived PFT data using the overlapped period. This correction has generated consistent PFT data across the sensors, therefore enabling the analyses of multi-year PFT observations by describing their variability and trends. Analysis of the two-decade time series of PFTs has revealed an increasing trend in diatoms and dinoflagellates and a decreasing trend in haptophytes and prokaryotic

20 phytoplankton on a global scale. The overall trend in green algae remains relatively stable, although with some spatial variations. These PFT trends are more significant in high latitudes and coastal regions, and for prokaryotic phytoplankton also in the equatorial region. Anomaly of PFTs in 2023 shows significant increases in Chla of diatoms and dinoflagellates (+24 % and +9.4 %, respectively), but only weak changes in Chla for prokaryotic phytoplankton (-2.1 %) and haptophytes (~1.6 %). These consistent time series data will act as an important ocean indicator to infer possible changes in the marine environment.

25 1 Introduction

Climate-induced changes stress the ocean's contemporary biogeochemical cycles and ecosystems, impacting the base of the marine food web - phytoplankton communities (Gruber et al., 2021). In the past decades, various observations of ocean color (OC) information, especially the chlorophyll *a* concentration (Chla) as a proxy of phytoplankton biomass, have been able to revolutionize our understanding of the marine biogeochemical processes and provide insights of the changes in phytoplankton

30 (e.g., Antoine et al., 2005; Gregg and Rousseaux, 2014; Behrenfeld et al., 2016). However, phytoplankton biomass cannot comprehensively describe the complex nature of the phytoplankton community, concerning their composition structure and function. Phytoplankton composition structure varies in ocean biomes and phytoplankton groups drive differently the marine ecosystem and biogeochemical processes (Bracher et al., 2017). Dedicated to marine biogeochemistry, continuous long-term monitoring of phytoplankton functional types (PFTs) with inter-annual variation and trend analysis will help understand better

35 the biogeochemical processes and benefit the assessment of ocean health (Xi et al., 2023).

Previously, we have developed and further improved an approach, referred to as EOF-PFT, consisting of a set of empirical-orthogonal-function based algorithms for the retrieval of PFTs on a global scale (Xi et al., 2020; 2021). Using multi-spectral remote sensing reflectance data (Rrs) from different OC satellites (GlobColour merged products and Sentinel-3A/B OLCI data) and sea surface temperature (SST) data, the EOF-PFT approach enables satellite retrievals of chlorophyll *a* concentration (Chla)

40 for five PFTs with pixel-by-pixel uncertainty, which include diatoms, dinoflagellates, haptophytes, green algae and prokaryotic



phytoplankton (prokaryotes hereafter for brevity). These PFT Chla products, covering the period from 2002 until today, are available on Copernicus Marine Service and updated regularly upon reprocessing with refined algorithms.

The PFT products enable the analyses of multi-year PFT observations by describing their variability and trends. However, prior to the time series analysis, the consistency of the PFT products derived from different sensors needs to be assured. In the frame of the Copernicus Marine Evolution Project GLOPHYTS, we aim to merge the PFT datasets of different sensors into one long-term consistent satellite PFT product. A first attempt has been carried out by Xi et al. (2023) with a correction scheme based on linear regressions with PFT uncertainty considered, which was applied to PFT data from Sentinel 3A/B OLCI sensors to generate PFT time series in the Atlantic Ocean. Though such a straightforward correction scheme provides an overall consistent time series, the spatial variation cannot be adequately corrected and large biases between sensors can still exist at regional scales. Therefore, we intend to enhance the correction skill by incorporating spatial variability. In this study, we propose a new correction scheme based on a random forest machine learning method for delivering two-decades quality-assured global PFT datasets, that are cross-validated within model training and further validated with in-situ data. The corrected PFT time series with high spatio-temporal consistency are analysed on both global and regional scales to investigate the trends and anomaly for different PFTs. For a longer goal, such PFT time series will further act as an important ocean indicator to help sustain the ocean health by providing inter-annual variation and trend analyses of the surface phytoplankton community structure, especially for the key regions that have been defined as vital marine environments by the Copernicus Marine Service.

2 Data and Methodology

2.1 PFT products from Copernicus Marine Service

The PFT datasets with per-pixel uncertainty (product ref. no. 1 in Table 1) have been generated by the EOF-PFT approach adapted based on the version proposed by Xi et al. (2021). The updated algorithms within EOF-PFT were developed using the latest global in situ pigment matchup dataset and trained separately for the merged OC products (including SeaWiFS, MODIS, MERIS and VIIRS) since 2002 with 8 bands and Sentinel 3A/B OLCI data (since May 2016) with 10 bands from GlobColour archive. The merged OC products rely on the current NASA release R2022 reprocessed version for MODIS and VIIRS (Table 8 in the QUID by Garnesson et al. 2023). The official PFT data (product ref. no. 1 in Table 1) are generated from the merged OC products for the period of July 2002–April 2016, and from OLCI products from May 2016 onwards. However, we extended PFTs products from the merged OC products to April 2017 in this study (product ref. no. 2 in Table 1), in order to have the one-year overlapping period with the OLCI-based PFT data for consistency analysis. The merged OC products were processed only until 2017 because VIIRS data from NASA release have been identified with significant trends (possibly due to degradation) after 2017 that are not identified in other sensors (e.g., Rrs at 443 nm with dramatic increase https://oceancolor.gsfc.nasa.gov/cgi/13bts?mssn=VIIRS&prod=Rrs_443&stat=AA&filt=1, other VIIRS product time series can also be checked via the link).

Updated EOF-PFT algorithms with the most up to date sensor reprocessing have also been assessed with an independent validation dataset with satisfactory performance (details in the corresponding updated QUID that will be available later this year). The corresponding prototypes have been prepared and will be implemented in the Copernicus Marine Service to generate reprocessed PFT products with per-pixel uncertainty through EiS (Enter into Service) by November 2024. With these updates, we obtained PFT retrievals still from two sensor sets, the merged OC sensor-derived and the OLCI sensor-derived PFTs. To generate long-term time series data and prepare for the next generation reprocessing, consistency between the PFT data across the two sensor sets must be assured.



Table 1: Products used.

Product ref. no	Product ID and type	Data access	Documentation
1	OCEANCOLOUR_GLO_BGC_L3_MY_009_103; satellite observations	EU Copernicus Marine Service Product (2024)	Quality Information Document (QUID): Garnesson et al. (2023); Product User Manual: Colella et al. (2023)
2	Self-processed PFT data based on merged OC products for the period of May 2016–April 2017 overlapped with the OLCI based PFT data available on the Copernicus Marine Service; satellite observations	Our own archive	Xi et al. (2021, 2023)
3	In situ PFT data; in situ observations	Our own archive	To be submitted to PANGAEA with a doi (Xi et al., 2024)

2.2 Machine Learning Based Ensemble (MLBE) for inter-sensor correction of PFT data

PFT data from the merged OC products have a longer timespan (~ 15 years) than the OLCI (Sentinel-3A/B) derived PFTs (~ 7 years) and are generated based on the algorithms trained with a larger global matchup dataset (~ 1500 data points compared to ~ 300 for OLCI due to its shorter running time and limited in situ data from 2016). The merged sensor-derived products also carry relatively lower uncertainty compared to the OLCI-derived PFT data. Therefore, we set up the modification scheme for the OLCI-derived PFTs to match the merged sensor-derived PFTs. A similar inter-sensor correction has been done for the OC-CCI merged OC data (Mélin and Franz, 2014; Sathyendranath et al., 2019). We tested a few machine learning methods (random forest, 1D-convolutional neural network, self-organizing map) to upgrade the OLCI-derived products consistency with the merged sensor-derived products on a pixel basis. At last, we used the random forest-based ensemble ‘TreeBagger’ with regression decision trees embedded in MATLAB (R2023b) which selects a subset of predictors for each decision split by the random forest algorithm to establish the correction model (Breiman, 2001). The ensemble is powerful in extracting spatial features from the predictors and establishing connections with the response variables through an optimal number of regression trees. Figure 1a shows a simplified flowchart of this machine learning ensemble, which is referred to as MLBE (Machine Learning Based Ensemble) hereafter. A brief description of the ensemble establishment is as follows.

- 1) Input data are the monthly PFT products derived from both merged sensor and OLCI data (May 2016 to April 2017, product ref. no. 2 in Table 1), from which the latitude, longitude, and PFT data from OLCI products during the 12 months are the predictor variables, and the PFT data from the merged sensors are response data. Only pixels with available data from both products were taken into account. The input dataset was randomly divided into training (70 %, ~3 million pixels) and testing dataset (30 %, ~1.26 million pixels). Before performing the training, latitude and longitude were normalised to [-1, 1], and natural log-transformed PFT data were normalised to [0, 1] so that these parameters are in Gaussian distribution.
- 2) The MLBE was trained separately for each PFT. After testing different numbers of regression trees for the training, we chose 30 regression trees to get the optimal training performance with relatively low computation cost (Fig. 1b). Trained models applied to the test datasets have shown equivalent performance with the training sets, indicating that the ensembles are robust.
- 3) The ensembles trained for the five PFTs (diatoms, haptophytes, dinoflagellates, prokaryotes and green algae) were applied to all monthly PFT products derived from OLCI from May 2016 to December 2023 to generate the corrected OLCI PFT data.



2.3 Validation data

We compiled two in situ datasets to validate the MBLE-corrected OLCI-derived PFT products (product ref. no. 3 in Table 1). Dataset 1 is the test dataset (99 matchups) extracted from the global in situ PFT matchup data, which takes up 30 % of the whole matchup dataset, while the other 70 % was used for the retuning of the PFT algorithm for OLCI sensors. Dataset 1 spans from 2016 to 2021 and spreads widely in the global ocean. Dataset 2 containing 134 matchups is a newly compiled dataset that composites in situ PFT data collected from four recent mostly polar expeditions with the research vessel *Polarstern* (Alfred-Wegener-Institut Helmholtz-Zentrum für Polar- und Meeresforschung, 2017), that are PS126 (May–June 2021), PS131/1 (June–Aug 2022) and PS136 (May–June 2023) in the north Atlantic to the Arctic Ocean, and PS133 (Oct–Nov 2022) in the Southern Ocean. Geographical distribution maps of the two datasets are included in Fig. 3 together with the validation plots. These matchup data will be made available upon publication on PANGAEA: <https://doi.org/10.1594/PANGAEA.xxxxxx>.

2.4 Trend and anomaly analysis

We focus on explorations of the consistent PFT products to reveal and understand the trends and variations of the global PFTs in the last two decades. We prepared time series on global scale and four regional scales including the North Atlantic Ocean, the Mediterranean Sea, the Arctic Ocean and the Southern Ocean. The other two regions of CMEMS's interest, the Baltic Sea and the Black Sea, were not included as the PFT algorithms were developed for open ocean waters (bathymetry > 200 m) and the quality of the PFT data generated in these regions cannot be assured (Xi et al., 2021). A deseasonalisation, referring to the process of removing the signal caused by seasonality from the time series, was first applied to the PFT time series. The deseasonalised time series were then prepared by decomposing the monthly data of each variable into a trend, seasonal and residual components with Seasonal-Trend decomposition using Loess (STL: Cleveland et al., 1990). Non-parametric Mann-Kendall test was used to identify statistically significant trends over time with p-value < 0.05 (Mann 1945, Kendall 1975, Gilbert 1987), and then the slope of the linear trend was estimated with the non-parametric Sen's slope (Sen, 1968). The standard deviation of the trend slope has been also calculated by considering PFT uncertainty assessed by the EOF-PFT retrieval algorithms. Time series analysis is done both, per-pixel and for the whole global ocean and selected regions. We detect trends reflected by the satellite observations and derive anomalies to observe the inter-annual changes. Anomalies of 2023 (the last year of the considered period) are also obtained following Xi et al. (2023) by comparing the PFT situation of 2023 to the mean of the last two decades.

3 Results

3.1 Correction of the OLCI-derived PFT data using the MLBE scheme

To reduce cross-sensor data shift and generate consistent PFTs, we have first applied a correction method while using the type II regression relationships with uncertainties included between the PFTs from merged data and that from OLCI data in the overlapped period, to correct the OLCI-derived PFT data to the merged data. The methodology was described in Xi et al. (2023). However, even though the final PFT time series over the global ocean shows good consistency, the difference between the two PFT products is still prominent in different regions. Taking the diatom product as a showcase, we calculated the relative difference (RD in %) between the OLCI-derived and merged sensor-derived diatom Chla using Equation (1). The median relative difference (MRD in %) over the globe was reduced significantly after the linear correction (from 45 % to 26 %), nevertheless, the RD can still reach as high as 80 %–100 % in different regions (figure not shown). High RD variations have also been found for other PFTs with the previously proposed correction scheme based on type II linear regression.

$$RD_{\text{diatom}} = (Chla_{\text{diatom}_{\text{OLCI}}} - Chla_{\text{diatom}_{\text{merged}}}) / Chla_{\text{diatom}_{\text{merged}}} * 100\%. \quad (1)$$



The scatterplot and statistics in Fig. 1d with the MLBE-corrected OLCI diatom Chla show significant improvement in consistency with the merged data diatom retrievals, compared to the non-corrected OLCI-derived diatom products (Fig. 1c). Figure 1f highlights the reduced RD variation over the global ocean compared to the RD between the non-corrected OLCI and merged-sensor-based PFTs shown in Fig. 1e. The slope of the corrected dataset is close to one, the median absolute difference (MAD) reduced from 0.13 mg m⁻³ to 0.02 mg m⁻³, and the median absolute relative difference (MARD) from 45 % to 5.7 %. The trained ensembles applied to the other four PFT products (haptophytes, dinoflagellates, prokaryotes, and green algae, see Fig. 2 for the global distribution of the RD for each) have also shown significant improvements with MAD of 0.002, 0.002, 0.003, 0.006 mg m⁻³, and MARD of 5.2 %, 4.2 %, 4.8 %, and 7.2 %, respectively. The MRD over the globe for all five PFTs is within ±1.5 % and shows no significant over-/underestimation.

The low RD observed for the overlapping year suggests that the MLBE correction scheme effectively aligns the OLCI-derived PFTs data with the merged sensor-derived PFTs, ensuring a strong spatial correspondence between the two datasets.

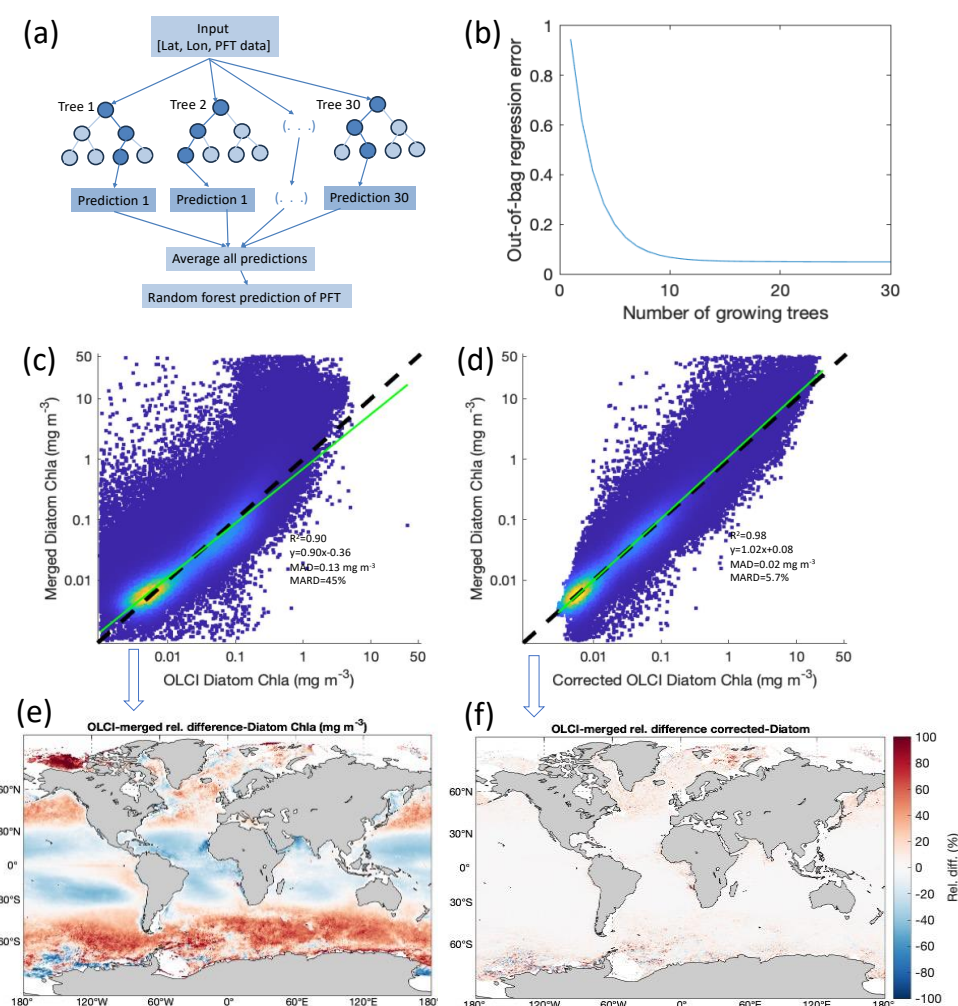


Figure 1: (a) Flowchart of the MLBE; (b) ensemble error with number of growing trees, scatterplots of (c) diatom Chla from OLCI non-corrected against that from merged products and (d) MLBE corrected OLCI diatom Chla against that from merged products, (e) RD between OLCI-based and merged sensor-based diatom Chla, and (f) RD between MLBE corrected OLCI-based and merged sensor-based diatom Chla.

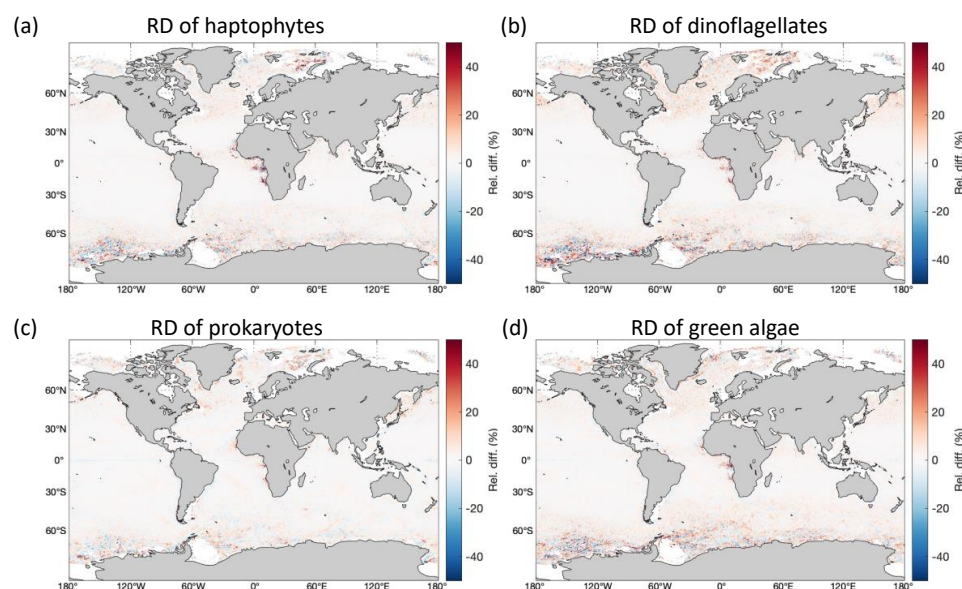


Figure 2: Global distribution of the RD between MLBE corrected OLCI and merged sensor-derived PFT Chla over one-year overlapped period (May 2016–April 2017).

3.2 Validation of the MLBE-corrected OLCI-derived PFT data

Scatterplots and statistics of the validation using dataset 1 (product ref. no. 3 in Table 1) displayed in Fig. 3a show good agreements between the corrected OLCI PFT data and the in situ ($R^2 > 0.45$), except for green algae. However, these scatterplots share a common feature – the cluster of data points with latitude $> 60^\circ$ N (light orange dots in Fig. 3a) are more off from the 1:1 line and thus show higher discrepancies than data points in other latitudes. The validation statistics for green algae has been strongly affected by these data in the Arctic waters. Despite of these Arctic data points, the overall validation shows that the MLBE correction on the OLCI derived PFT data keeps the distribution features of these PFTs, indicating its potential to generate consistent time series data. Unsurprisingly, validation using dataset 2, that contains recently obtained in situ data in high latitudes only, has exhibited larger discrepancies than that from dataset 1 (Fig. 3b). Only diatoms, dinoflagellates and prokaryotes show significant correlation but with low R^2 (0.15–0.26). Corrected haptophytes showed a narrower variation range (0.03–0.3 mg m^{-3}) compared to the in situ data (0.01–1.8 mg m^{-3}). Prokaryotes and green algae show underestimations from the corrected OLCI data compared to the in situ, mostly for the Arctic data. This confirms once more that PFT data in high latitudes bear large uncertainties, which is in line with the per-pixel uncertainty estimated by considering errors induced by the input satellite data and the EOF-PFT algorithm parameters. Phytoplankton observation in the high latitudes, particularly the Arctic Ocean, needs more attention in terms of improved estimation methods and higher data quality.

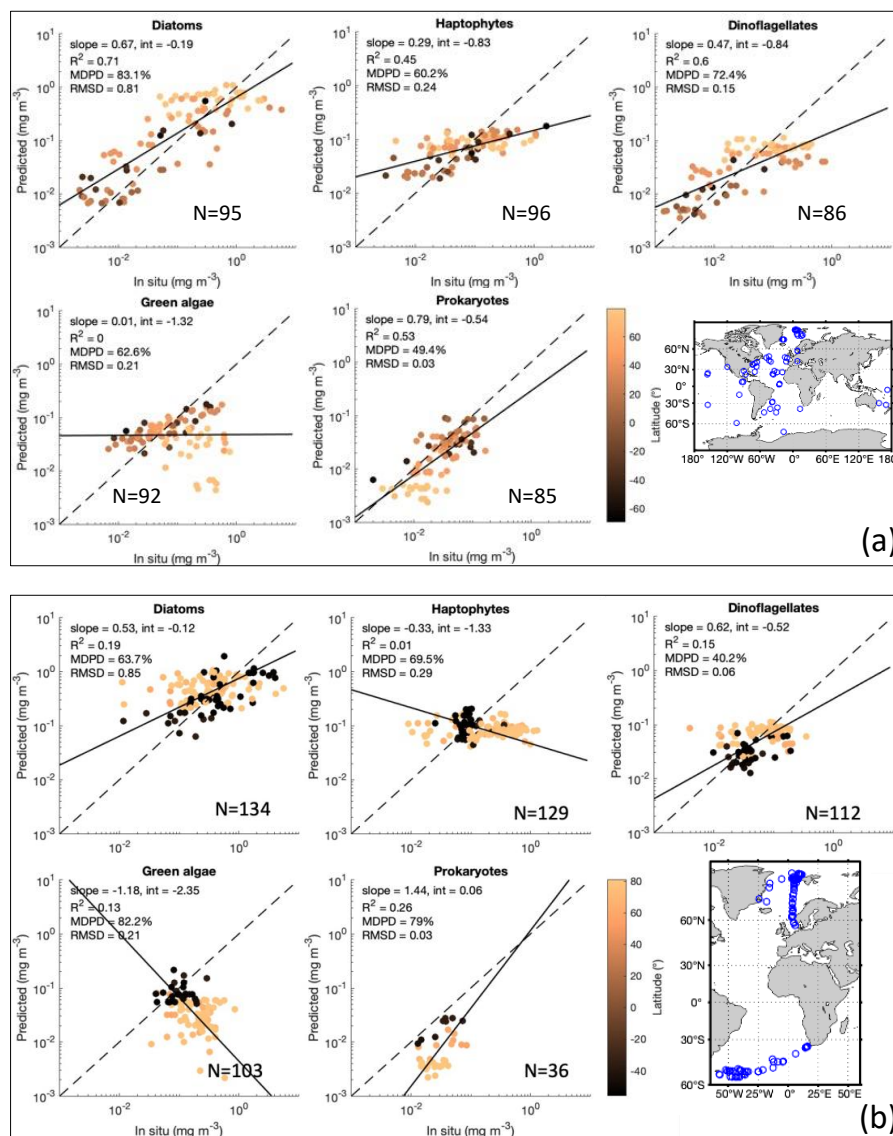


Figure 3: Panel (a): MLBE-corrected PFT Chla from OLCI sensors in comparison with in situ PFT dataset 1. Panel (b): same as the validation in Panel A, but using in situ PFT dataset 2. Map of the data distribution for datasets 1 and 2 (product ref. no. 3 in Table 1) are shown in each panel respectively.

3.3 PFT time series analysis

We applied the MLBE correction scheme on global scale to the OLCI monthly products and generated time series for the five PFTs from July 2002 to December 2023. With the corrections applied to OLCI data, all five PFTs show very consistent time series (Fig. 4a). The MLBE corrected OLCI PFT data and the merged PFT data have shown almost identical values during the overlapped period (May 2016–April 2017). Only for green algae the correction is slightly less satisfactory than the others, which should be due to the weaker correlation ($R^2 < 0.7$) between the original OLCI and merged sensor derived PFT data whereas the other four PFTs show R^2 all above 0.9. This weaker correlation for green algae has subsequently led to reduced performance in the MLBE correction, which has been reflected in the validation in Fig. 3 as well.



The PFT time series have been analysed at the global scale and four regional scales including the North Atlantic Ocean, the Mediterranean Sea, the Arctic Ocean and the Southern Ocean. Figure 4b shows the time series with slopes indicating the PFT trends per decade and the corresponding slope errors for all the PFTs at different scales. Figure 5 shows the significant PFT trends (p -value < 0.05) on a pixel basis over the globe to have a better understanding of the spatial distribution of the trends.

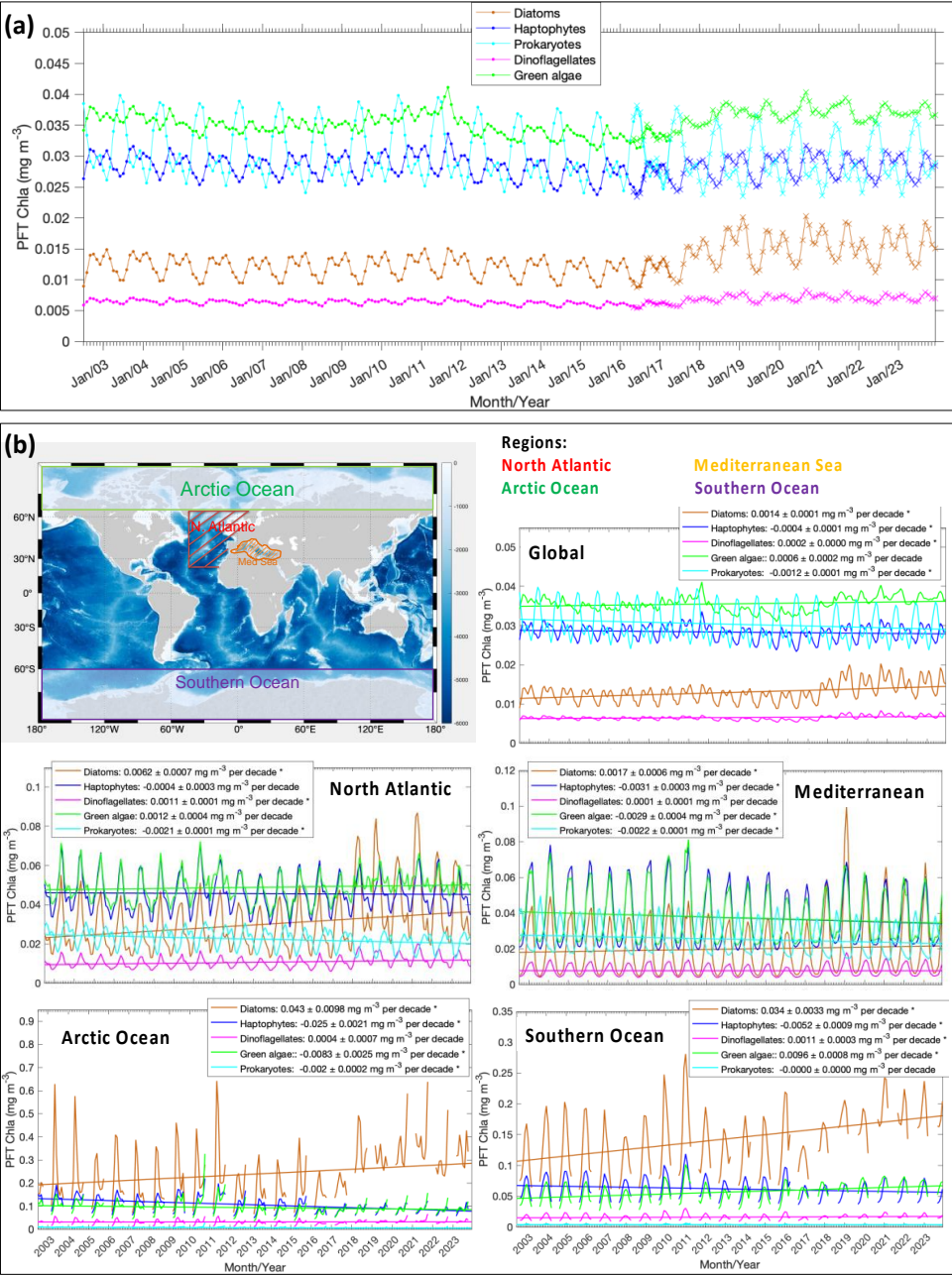
Diatoms show a significant increasing trend for the global ocean and selected regions, especially in the Atlantic section of the polar regions (Fig. 5a). Further, a distinct increase has been found in more recent years since autumn 2017 and is still prominent in 2023. The global trend of diatom Chla is increasing by $0.0014 \pm 0.0001 \text{ mg m}^{-3}$ per decade and with a dramatic increase in the polar regions (0.034 and 0.043 mg m^{-3} per decade for the Southern Ocean and the Arctic Ocean, respectively). This overall increasing trend is mainly driven by the significant elevation in diatom biomass observed since late 2017, whereas the time series from 2002 to summer 2017 shows relatively stable diatom biomass.

Haptophytes Chla exhibits a slight decrease in general on the global scale ($-0.0004 \pm 0.0001 \text{ mg m}^{-3}$ per decade) and all other regional zones but the decrease is not significant in the North Atlantic Ocean. Global per-pixel trend (Fig. 5b) shows a more significant decrease in coastal areas, the sub-Arctic and Arctic regions, and high variability in the Southern Ocean with an overall decrease.

Dinoflagellates show a similar pattern with diatoms, i.e., a significant increasing trend ($0.0002 \pm 0.0000 \text{ mg m}^{-3}$ per decade) in the last two decades mainly driven by the increase in dinoflagellates Chla since mid-2017, but their biomass is still low compared to other PFTs as they are usually undominant in the phytoplankton community composition. No significant trends have been found for dinoflagellates biomass in the Mediterranean Sea and the Arctic Ocean.

Green algae show no significant trend on the global scale. The time series show a less obvious seasonal pattern than the other PFTs, possibly due to that they are barely the dominant group in the global ocean and mostly co-exist with the other PFTs which show clear dominance in certain regions at specific times, depending on their ecological features. The biomass reached its peak in October 2011, followed by a few years of decrease but started to increase in 2018. On the regional scale, a slight decrease in the Mediterranean Sea and the Arctic Ocean, and a slight increase in the Southern Ocean have been observed, which is shown in the per-pixel trend (Fig. 5d). The decreasing trend is seen in coastal regions such as the north European coastlines, the west coast of America and Africa, and the north coast of the Arabian Sea.

Prokaryotes Chla displays an overall significant decreasing trend on the global scale ($-0.0012 \pm 0.0001 \text{ mg m}^{-3}$ per decade) and the selected regional zones except for the Southern Ocean. Global per-pixel trend (Fig. 5e) shows that the north hemisphere with significant decrease near the equator within $15^\circ \text{ S} - 25^\circ \text{ N}$ (Indian Ocean, West Africa, low latitudes in the Pacific Ocean), but a slight increase is shown in the belt of $15^\circ \text{ S} - 35^\circ \text{ S}$. Very mild changes have been found in high latitudes where they have generally low Chla.



225 **Figure 4. Panel (a):** Updated (corrected) time series of the five PFT Chla based on the global mean from 2002 to 2023. Merged
products cover the period of July 2002–April 2017 (indicated with dots), and OLCI products are for May 2016–Dec 2023 (indicated
with crosses). Note that the OLCI products have been corrected to merged products based on MLBE. Panel (b): Trends of diatoms,
haptophytes, dinoflagellates, green algae and prokaryotes Chla on the global scale and four regional scales (the North Atlantic
Ocean, the Mediterranean Sea, the Arctic Ocean and the Southern Ocean), respectively. Trend slopes per decade with uncertainties
230 have been indicated with significant trends marked with an asterisk (*).

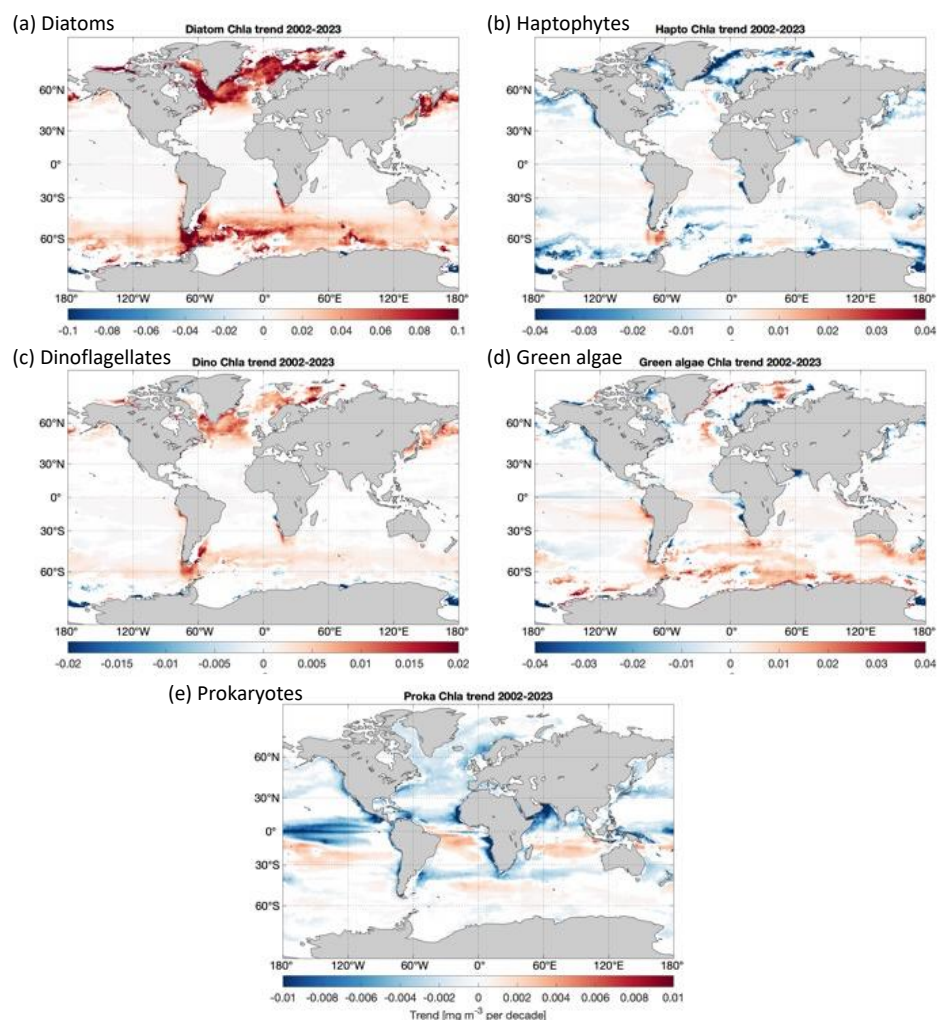


Figure 5. Per-pixel trends for Chla of (a) diatoms, (b) haptophytes, (c) dinoflagellates, (d) green algae, and (e) prokaryotes (only where $p < 0.05$ is shown; slope unit: mg m^{-3} per decade).

3.4 PFT anomaly of 2023

Figure 6 shows the relative anomalies (%) of the five PFTs in 2023 compared to the average PFT state over the 20 years. The diatom anomaly presents higher Chla for most of the global ocean with a dramatic increase in latitudes $> 40^\circ$. This can already be expected from the time series in Fig. 4a where diatoms show elevated Chla since autumn 2017 and keep similar higher biomass in 2023. The global mean of the diatom in 2023 is about 24 % higher than the two-decade average, and the anomaly varies from -30% to 110 % with extremely high values in the Arctic Ocean and the coastal regions in the southern part of South America. Dinoflagellates show a similar anomaly with diatoms in a much milder pattern, which has a global mean of about 9.4 %. The haptophyte anomaly presents changes without a clear pattern, showing slight increases in Chla in the Pacific gyres, eastern Indian Ocean and the Southern Ocean, but slight decreases in the temperate latitudes. The overall global mean anomaly of haptophytes Chla is only very slightly higher compared to the two-decade average (1.6 %). Green algae show a similar distribution in biomass change as haptophytes but a bit more prominent increase in most of the global oceans (global mean of 6.5 %). Prokaryotes show in general decreased Chla in 2023 (global mean of -2.1 %), with only slight increases observed in the South Pacific Ocean and part of the Southern Ocean.

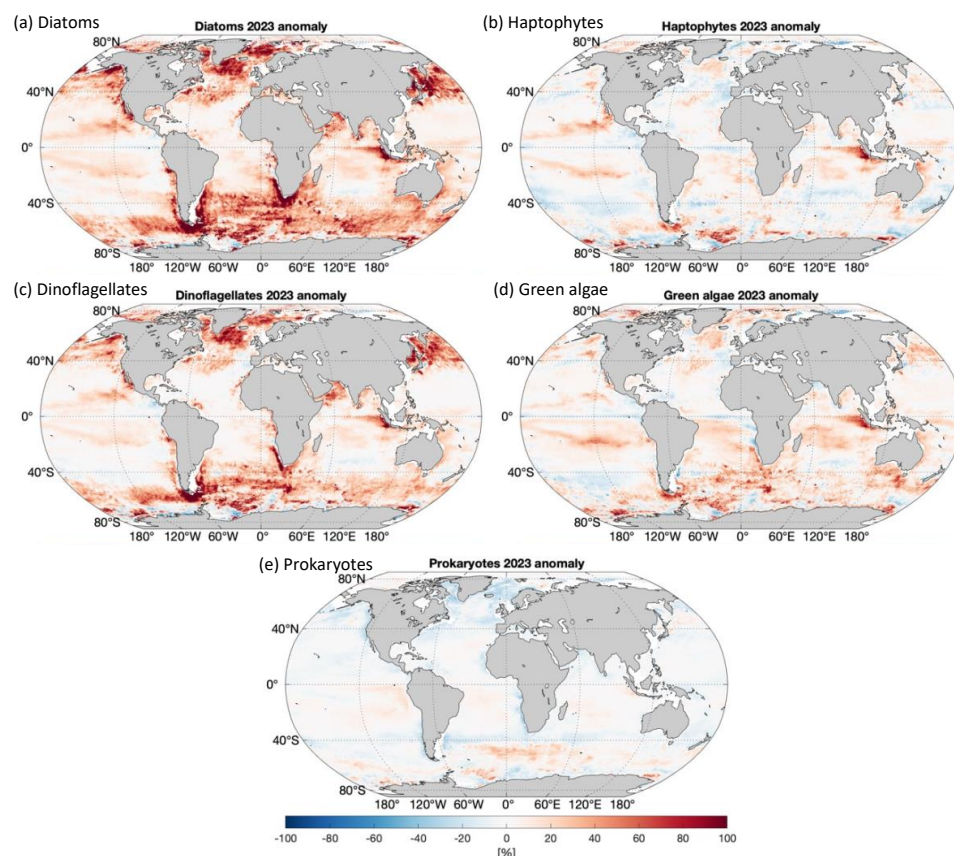


Figure 6. Relative anomaly of 2023 for Chla of (a) diatoms, (b) haptophytes, (c) dinoflagellates, (d) green algae, and (e) prokaryotes.

250 4 Discussion, conclusions and outlook

This study aims to demonstrate consistent PFT time series data on the global scale and for the polar regions and the European Seas which were developed based on a robust machine learning correction scheme. The proposed MLBE correction scheme outperforms the previously proposed method that was based on type II linear regression with considerations of PFT uncertainties (Xi et al., 2023). For the overlapping period, the MLBE scheme demonstrates high consistency of the corrected
 255 OLCI derived PFTs to the merged sensor derived PFTs, both in space and time, increasing our confidence in employing the data for further time series studies.

The time series generated based on the consistent PFT data on the global scale from 2002 to 2023 has shown a clear increasing trend for diatoms and dinoflagellates, and a slight decreasing trend for haptophytes and prokaryotes, while the green algae exhibit no significant trend. To date, the longest time series for ocean color products still covers less than three decades (starting
 260 in 1997 with the launch of SeaWiFS). Though it may still not be long enough for a robust trend analysis due to too strong decadal variability (Henson et al. 2010; Henson et al., 2016), these time series can help to catch distinct changes on different scales by comparing to the climatological state. Indeed, the findings such as significant increase in diatoms particularly after 2017 are of interest to in-depth investigations linking climate drivers to such prominent changes. For instance, potential responses of phytoplankton biomass to increasingly frequent marine heat waves in the past years can be a suitable starting
 265 point. More field observations on phytoplankton community composition are also now in collection for necessary evaluations and hypothesis verifications.



Changes in phytoplankton biomass have been described by the chlorophyll *a* concentration derived from ocean color satellites covering the last decades. Trends of the Chl_a at different scales can be generated using current operational chlorophyll products such as OC-CCI and GlobColour. For instance, Chl_a as an OMI has been included by the Copernicus Marine Service where the climate trends of various OMIs are provided to indicate the state of the ocean health. The current published time series of Chl_a shows in general an increase during 1997–2022 on the global scale and also for the North Atlantic and Arctic regions. The published per-pixel Chl_a trend map shows a more prominent increasing trend in high latitudes but a slight decrease in mid- to low latitudes (e.g., <https://doi.org/10.48670/moi-00230>). These trends are in good agreement with our PFT time series which shows an overall increasing trend of the total biomass mainly due to the increased diatom biomass. Similar findings on both global and regional scales have been reported by Van Oostende et al. (2023), where the OC-CCI dataset has been used but with careful consideration of the spatiotemporal coverage of the different sensor datasets by applying a temporal gap detection method. Other techniques such as gap filling and statistical temporal decomposition are also in demand for more robust PFT data analysis, to increase the accuracy in separating the long-term signal from the seasonal component of the time series.

Validation has been performed at different levels from the model development stage (details not shown in this study) to the corrected OLCI derived PFT data to understand well the reliability of the datasets. Using validation data covering different times and regions, we observed that the satellite PFT data have larger discrepancies from the in situ data in high latitudes especially in the Arctic Ocean, which has been also reflected in the per-pixel uncertainty assessment for the EOF-PFT algorithm (Xi et al., 2021). However, our validation for diatoms and dinoflagellates in the Arctic Ocean using dataset 2, collected during 2021–2023, shows no overestimation of the satellite retrievals though overall a weak correlation, indicating that our satellite retrievals indicate correctly the increased biomass for the two PFTs. Since the ecosystem in the Arctic Ocean undergoes fast changes as a consequence of the arctic warming and sea ice retreat, there are still a lot of unknowns on how the phytoplankton community adapts and responds to these changes (Oziel et al., 2018; Meredith et al., 2019). It is potentially essential for the Copernicus Marine Service to provide not only for the white ocean but also for the green ocean a wide range of biological/biogeochemical variables to better understand the state and possible tendencies of the ecosystems in the Arctic Ocean.

This work is at the cutting-edge attempting to demonstrate the most up-to-date long-term phytoplankton community in several functional groups derived from ocean color products. Providing inter-annual variation and trend analyses of the surface phytoplankton community structure, the PFT will complement the chlorophyll products on the Copernicus Marine Service as an essential ocean variable and help in the assessment of the ocean health in the biogeochemical aspect.

Data availability

Data and products used in this study and their availabilities and supporting documentations are listed in Table 1. In situ HPLC pigment and PFT data used for validation will be available on PANGAEA upon publication (<https://doi.org/10.1594/PANGAEA.xxxxxx>).

Author Contributions

HX, AB, MB and AM conceptualized the study. HX designed and carried out the experiments. MB and JD provided support in satellite products and matchup data extraction. EM contributed to the machine learning algorithms. HX drafted and revised the manuscript with contributions from all co-authors.



Competing interests

305 The authors declare that they have no conflict of interest.

Acknowledgments

We thank the two Copernicus Marine – Innovation Service Evolution R&D Projects, GLOPHYTS (2022-2024) and ML-PhyTAO (2024-2026), for funding. Copernicus Marine Service is implemented by Mercator Ocean International in the framework of a delegation agreement with the European Union. This work was also partly supported by DFG (German Research Foundation) Transregional Collaborative Research Center ArctiC Amplication: Climate Relevant Atmospheric and SurfaCe Processes, and Feedback Mechanisms (AC)3 (Project C03), and the ESA project 4DMED-Sea (4000141547/23/I-DT). Ehsan Mehdipour’s work was supported by the project “4D-Phyto” funded by AWI-INSPIRES and HGF-MarDATA. Thanks to ESA, EUMETSAT and NASA for distributing ocean color satellite data, and especially to the ACRI-ST GlobColour team for providing OLCI and merged ocean colour L3 products. In situ data from four *Polarstern* expeditions were funded under Grants AWI_PS126_02, AWI_PS131_5, AWI_PS133/1_11 and AWI_PS136_04, respectively. Captain, crew, and expedition scientists are also acknowledged for their support at sea.

References

- Alfred-Wegener-Institut Helmholtz-Zentrum für Polar- und Meeresforschung: Polar Research and Supply Vessel POLARSTERN Operated by the Alfred-Wegener-Institute, Journal of large-scale research facilities, 3, A119, <http://dx.doi.org/10.17815/jlsrf-3-163>, 2017.
- Antoine, D., Morel, A., Gordon, H. R., Banzon, V. F., and Evans, R. H.: Bridging ocean color observations of the 1980s and 2000s in search of long-term trends, *J. Geophys. Res. Oceans*, 110, C06009, <https://doi.org/10.1029/2004JC002620>, 2005.
- Behrenfeld, M. J., O’Malley R. T., Boss, E. S., Westberry, T. K., Graff, J. R., Halsey, K. H., Milligan, A. J., Siegel, D. A., and Brown, M. B.: Revaluating ocean warming impacts on global phytoplankton, *Nat. Clim. Change*, 6, 3223–3330, <https://doi.org/10.1038/nclimate2838>, 2016.
- Bracher, A., Bouman, H. A., Brewin, R. J. W., Bricaud, A., Brotas, V., Ciotti, A. M., Clementson, L., Devred, E., Di Cicco, A., Dutkiewicz, S., Hardman-Mountford, N. J., Hickman, A. E., Hieronymi, M., Hirata, T., Losa, S. N., Mouw, C. B., Organelli, E., Raitsos, D. E., Uitz, J., Vogt, M., and Wolanin, A.: Obtaining phytoplankton diversity from ocean color: a scientific roadmap for future development, *Front. Mar. Sci.*, 4, 1–15, <https://doi.org/10.3389/fmars.2017.00055>, 2017.
- Breiman, L.: Random Forests, *Machine Learning*, 45, 5–32, <https://doi.org/10.1023/A:1010933404324>, 2001.
- Cleveland, R. B., Cleveland, W. S., McRae, J. E., and Terpenning, I.: STL: A seasonal-trend decomposition procedure based on Loess, *J. Official Statistics*, 6(1), 3–73, https://doi.org/10.1007/978-1-4613-4499-5_24, 1990.
- Colella, S., Böhm, E., Cesarini, C., Garnesson, P., Netting, J., and Calton, B.: EU Copernicus Marine Service Product User Manual for Ocean Colour Products, Issue 3.0, Mercator Ocean International, <https://catalogue.marine.copernicus.eu/documents/PUM/CMEMS-OC-PUM.pdf> (last access: 22 Aug 2024), 2023.
- Garnesson, P., Mangin, A., Bretagnon, M., and Jutard, Q.: EU Copernicus Marine Service Quality Information Document (QUID) for OC TAC Products OCEANCOLOUR OBSERVATIONS GlobColour, Issue 4.0, Mercator Ocean International, <https://catalogue.marine.copernicus.eu/documents/QUID/CMEMS-OC-QUID-009-101to104-111-113-116-118.pdf> (last access: 22 Aug 2024), 2023.
- Gilbert, R. O.: Statistical Methods for Environmental Pollution Monitoring. John Wiley and Sons, United States, 336 pp., 1987.
- Gregg, W. W. and Rousseaux, C. S.: Decadal trends in global pelagic ocean chlorophyll: A new assessment integrating multiple satellites, in situ data, and models, *J. Geophys. Res. Oceans*, 119, 5921–5933, <https://doi.org/10.1002/2014JC010158>, 2014.



- Gruber, N., Boyd, P. W., Frölicher T. L., and Vogt, M.: Biogeochemical extremes and compound events in the ocean, *Nature*, 600, 395–407, <https://doi.org/10.1038/s41586-021-03981-7>, 2021.
- 345 Henson, S. A., Beaulieu, C., and Lampitt, R.: Observing climate change trends in ocean biogeochemistry: when and where, *Glob. Chang. Biol.*, 22(4), 1561–1571, <https://doi.org/10.1111/gcb.13152>, 2016.
- Henson, S. A., Sarmiento, J. L., Dunne, J. P., Bopp, L., Lima, I., Doney, S. C., John, J., and Beaulieu, C.: Detection of anthropogenic climate change in satellite records of ocean chlorophyll and productivity, *Biogeosci.*, 7, 621–640, <https://doi.org/10.5194/bg-7-621-2010>, 2010.
- 350 Kendall, M. G.: Rank Correlation Methods, *Journal of the Institute of Actuaries*. 75 (1), 140–141, <https://doi.org/10.1017/S0020268100013019>, 1948.
- Mann, H. B: Nonparametric tests against trend. *Econometrica* 13, 245, <https://doi.org/10.2307/1907187>, 1945.
- Mélin, F. and Franz, B. A.: Chapter 6.1 – Assessment of satellite ocean colour radiometry and derived geophysical products, *Experimental Methods in the Physical Sciences*, 47, 609–638, <https://doi.org/10.1016/B978-0-12-417011-7.00020-9>, 2014.
- 355 Meredith, M., Sommerkorn, M., Cassotta, S., Derksen, C., Ekaykin, A., Hollowed, A., Kofinas, G., Mackintosh, A., Melbourne-Thomas, J., Muelbert, M. M. C., Ottersen, G., Pritchard, H., and Schuur, E. A. G.: Polar Regions, In: IPCC Special Report on the Ocean and Cryosphere in a Changing Climate, edited by: Pörtner, H.-O., Roberts D. C., Masson-Delmotte V., Zhai P., Tignor M., Poloczanska E., Mintenbeck K., Alegria A., Nicolai M., Okem A., Petzold J., Rama B. and Weyer N.M., Cambridge University Press, Cambridge, UK and New York, NY, USA, 203–320, <https://doi.org/10.1017/9781009157964.005>, 2019.
- 360 Oziel, L., Baudena, A., Ardyna, M., Massicotte, P., Randelhoff, A., Sallée, J. -B., Ingvaldsen, R. B., Devred, E., and Babin, M: Faster Atlantic currents drive poleward expansion of temperate phytoplankton in the Arctic Ocean, *Nature Comm.*, 11, 1705, <https://doi.org/10.1038/s41467-020-15485-5>, 2020.
- Sen, P. K.: Estimates of the regression coefficient based on Kendall’s tau, *J. Am. Stat. Assoc.*, 63, 1379–1389, <https://doi.org/10.1080/01621459.1968.10480934>, 1968.
- 365 Sathyendranath, S., Brewin, R. J. W., Brockmann, C., Brotas, V., Calton, B., Chuprin, A., Cipollini, P., Couto, A. B., Dingle, J., Doerffer, R., Donlon, C., Dowell, M., Farman, A., Grant, M., Groom, S., Horseman, A., Jackson, T., Krasemann, H., Lavender, S., Martinez-Vicente, V., Mazeran, C., Mélin, F., Moore, T. S., Müller, D., Regner, P., Roy, S., Steele, C., Steinmetz, F., Swinton, J., Taberner, M., Thompson, A., Valente, A., Zühlke, M., Brando, V. E., Feng, H., Feldman, G., Franz, B. A.,
- 370 Frouin, R., Gould, R. W., Hooker, S. B., Kahru, M., Kratzer, S., Mitchell, B. G., Muller-Karger, F. E., Sosik, H. M., Voss, K. J., Werdell, J., and Platt, T.: An ocean-colour time series for use in climate studies: The experience of the Ocean-Colour Climate Change Initiative (OC-CCI), *Sensors*, 19, 4285, <https://doi.org/10.3390/s19194285>, 2019.
- van Oostende, M., Hieronymi, M., Krasemann, H., and Baschek, B.: Global ocean colour trends in biogeochemical provinces, *Front. Mar. Sci.*, 10, 1052166, <https://doi.org/10.3389/fmars.2023.1052166>, 2023.
- 375 Xi, H., Losa, S. N., Mangin, A., Soppa, M. A., Garnesson, P., Demaria, J., Liu, Y., d’Andon, O. H. F., and Bracher, A.: A global retrieval algorithm of phytoplankton functional types: Towards the applications to CMEMS GlobColour merged products and OLCI data, *Remote Sensing of Environment*, 240, 111704, <https://doi.org/10.1016/j.rse.2020.111704>, 2020.
- Xi, H., Losa, S. N., Mangin, A., Garnesson, P., Bretagnon, M., Demaria, J., Soppa, M. A., d’Andon, O. H. F., and Bracher, A.: Global chlorophyll a concentrations of phytoplankton functional types with detailed uncertainty assessment using multi-sensor
- 380 ocean color and sea surface temperature satellite products, *Journal of Geophysical Research-Oceans*, 126(5), <https://doi.org/10.1029/2020JC017127>, 2021.
- Xi, H., Bretagnon, M., Losa, S. N., Brotas, V., Gomes, M., Peeken, I., Alvarado, L. M. A., Mangin, A., and Bracher, A.: Satellite monitoring of surface phytoplankton functional types in the Atlantic Ocean over 20 years (2002–2021), Contribution to the 7th edition of Copernicus Marine Service Ocean State Report, State of the Planet, 1-osr7, 5, [https://doi.org/10.5194/sp-](https://doi.org/10.5194/sp-1-osr7-5-2023)
- 385 [1-osr7-5-2023](https://doi.org/10.5194/sp-1-osr7-5-2023), 2023.